

Large-Expansion Bi-Layer Auxetics Create Compliant Cellular Motion

Lillian Chin,^{1,2}, Gregory Xie¹, Jeffrey Lipton,^{1,3}, Daniela Rus¹

Abstract— There is significant interest in creating compliant modular robots that can change their volume. Inspired by how biological cells move, these systems can potentially combine the resilience of modular robotics with the increased environmental interactions of soft robotics. However, current versions have limited speed, expansion, and portability. In this paper, we address these concerns through AuxSwarm, a compliant system composed of auxetic-based robotic voxels. These voxels control their volume through a scissor-like bi-layer auxetic design, growing up to 1.57 times their original size in 0.2 seconds. This combination of speed and expansion is unique across modular soft robots, enabling dynamic locomotion capabilities. We characterize the voxels and demonstrate the versatility of this approach through case studies of 2D bending and 3D cube flipping. AuxSwarm provides a first step towards addressable voxel-based smart materials, while simultaneously addressing the robustness and actuation challenges faced by soft robots.

I. INTRODUCTION

Creating compliant modular robotic systems has been a longstanding goal of the robotics community. Inspired by nature’s hierarchy of cells and tissues, “programmable matter” leverages the motions of its individual modules to create large-scale global behavior [1]. Programmable matter adds new dynamic environmental intelligence to everyday objects, especially when combined with soft robotics. Independently addressing unit cells of a larger compliant system could cause more controlled and selective interactions with the environment than current soft robotics’ bulk movement [2].

Although modular robotics has demonstrated many successes in the rigid realm [3], translating these to the soft robotics realm has remained difficult. Most soft modular robots combine fluid-based actuators with connectors to produce a compliant robot with a centralized hard core for power, pressure, and control [4]–[6]. Others distribute the control hardware, dispersing rigid connections throughout the soft robotic structure [7, 8]. Since all of these robotic materials rely on air-driven expansion, these systems often require tethers to a large external pressure source with slow actuation times, often on the order of 30-60 s [9]. [10] offers a notable exception by providing an untethered inflatable structure with tunable material properties and significant force output, but still suffers from a long actuation time. Soft robots’ deformability also means that modular systems have largely been demonstrated in planar-only contexts [5,

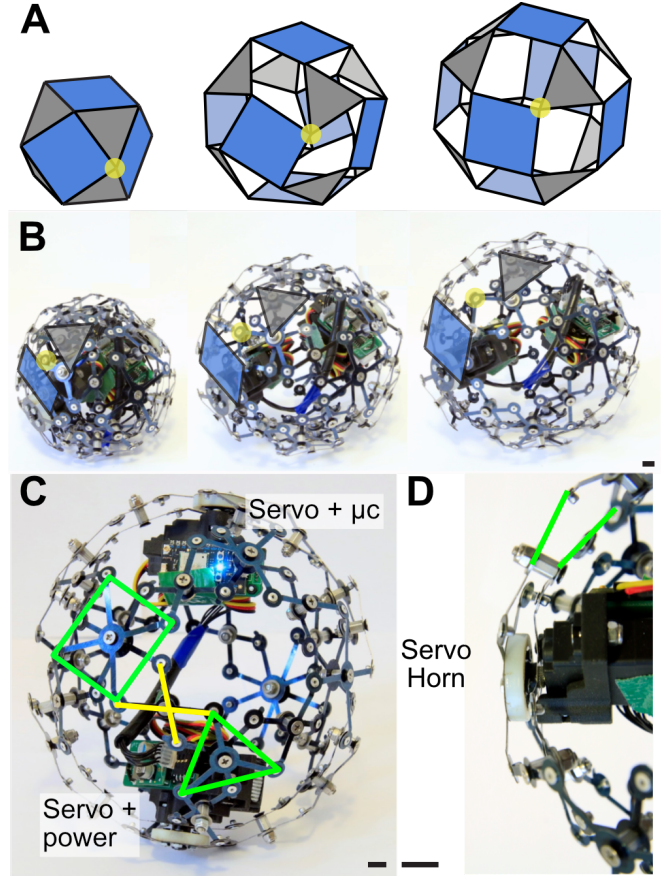


Fig. 1. The AuxSwarm’s individual units build off of (A) the jitterbug expansion pattern. The voxels replace the pin-joint rotations (yellow circle) with (B) a scissor-link joint to maximize expansion. (C) Schematic overlay highlighting the rotating polygons (green) and the scissor-link mechanism (yellow). (D) Close-up of the servo’s connections to the auxetic shell, demonstrating how the two layers (green) are offset from one another, allowing for the scissor action to occur. Scale bars are 1 cm.

10, 11], unlike the multi-dimensional structures seen in rigid systems [12, 13]. There is a clear need for compliant systems that remain as easy to control as rigid modular robots.

We address this need through AuxSwarm, a compliant modular robotics system composed of auxetic voxels. Building on our previous work on modular auxetic robots [14, 15] and inspired by more mechanisms-based approaches to soft robotics [16], AuxSwarm uses spring steel in a unique bi-layer scissor link mechanism for direct and quick control over the voxel’s expansion. Each voxel is capable of a large radial expansion (1.57×) in a very short amount of time (0.2 seconds). To the best of our knowledge, this is the fastest expansion rate shown for soft robotic modules. We achieve this speed by driving the linkages directly with a motor rather than pneumatics or linear actuators. Combining this direct

¹Computer Science and Artificial Intelligence Laboratory, Massachusetts Institute of Technology, Cambridge, MA 02139, USA

²Department of Electrical and Computer Engineering, The University of Texas at Austin, Austin, TX 78712, USA

³Department of Mechanical and Industrial Engineering, Northeastern University, Boston, MA 02115, USA

Correspondence: ltchin@utexas.edu

drive with spring steel allows each voxel to expand quickly while maintaining a stiffness comparable to other soft robots (280 – 388 N/m). A voxel’s local compliance is matched with flexible voxel-voxel connections that can accommodate the voxels’ expansion. This structure gives AuxSwarm a local and global compliance while simultaneously having the predictability of a motor-driven design.

We make the following contributions

- 1) Design of the auxetic bi-layer scissor mechanism
- 2) Creation of an expanding voxel using that mechanism
- 3) Characterization of the voxel, demonstrating the fastest expansion rate for soft robotic modules
- 4) Composition of the voxels into an 8-voxel AuxSwarm, with demonstration of 2D bending and 3D locomotion

II. UNIT CELL DESIGN AND FABRICATION

In our previous work [14, 15], we demonstrated how the geometry of auxetic shells enables a single degree-of-freedom (DoF) control over a structure’s expansion. To summarize that work, we recreated Buckminster Fuller’s “jitterbug” structure by arranging squares and triangles faces into a cuboctahedron that expand to form a rhombicuboctahedron [17]. Fig. 1A demonstrates how the jitterbug structure turns face-face rotation into overall expansion. In other words, the angle between two faces is the single DoF that determines how the structure moves through its “auxetic trajectory” to expand fully. Rather than actuate this rotation directly, we used a motorized leadscrew to push antipodal points away from each other while allowing for face-face rotations.

While these previous iterations were multiple orders of magnitude faster than other volume-changing modular robots (Tab. 4 of [15]), the reliance on a rigid leadscrew meant that compliance and expansion ratio were sacrificed for higher force output. Our previous work also required external constraints to achieve locomotion, like a tube to push against or a wire to bend inwards. We would like this newer iteration to prioritize size, speed and compliance for more soft and dynamic applications.

A. Auxetic Shell

The main technical innovation of this paper is the use of a *bi-layer scissor* design for the auxetic shell (Fig. 1B). Specifically, our voxels use a servo to directly counter-rotate two jitterbug-style shells against one another, effectively creating a scissor linkage in between each rotation point. This avoids many of the previous limitations to expansion ratio seen in [14] while maintaining the compliance that was sacrificed in [15].

This new design was inspired by expandohedra, a class of expanding polyhedra structures described in [18, 19]. These models are theoretically able to expand to $1.77 \times$ their original radius by placing a thick rotating link along the sides of polyhedral structures attached at axes at an angle to the face polygons. Effectively, rather than having a single point of contact for the rotation like the jitterbug, the expandohedra adds a single line of extension. That way, as the polygonal sides rotate, the link goes from being along the

side of the polygon to an angle normal to them, providing extra expansion. However, these links add additional DoF and make the structure unstable.

To preserve the single DoF nature of the shell, we take the expandohedra model and layer its mirror image. By offsetting the mirror images from one another and introducing connections between the layers at the midpoint of the rotating links, we effectively create a scissor mechanism between the faces (Fig. 1C). This allows for extra expansion while maintaining the single DoF nature of the auxetic trajectory. If the outer and inner layers align, the structure becomes degenerate and we recover the original version of the unstable expandohedra. Theoretically, we could insert this scissor mechanism as many times between the joints as desired, but this comes at the cost of introducing more effective slop between the rotating polygons, creating an overall weaker structure.

This bi-layer scissor design presents several advantages. First, offsetting the two layers avoids the intersection issues seen in [14] that limited the level of expansion, putting this design more on par with other soft modular robots. Secondly, the bilayer design allows for the direct actuation by inducing rotation between the layers. This direct control over the auxetic trajectory’s DoF also allows us to achieve a large expansion in a small amount of time, enabling us to impart a large impulse on the environment.

To maintain compliance, we built our auxetic shell out of 2.5 mm wide spring steel struts, laser cut out of 0.254 mm thick spring steel. Spring steel gave us a good trade-off between the strength needed to rotate about a pin joint while also giving a general compliance to the AuxSwarm. The ends of each strut were bent at 20° to form the overall curvature of the shell and had tabs to prevent reaching the degenerate alignment case. The two shell layers were spaced apart with 6 mm standoffs and were held against the standoff with a M3 bolt and locknut. Each of the pins of the pin joints were made with 2 mm rivets.

B. Actuation and Control

Since the modified expandohedra shell ties rotation with volumetric expansion, we can control the size of an AuxSwarm voxel through direct rotations of the internal polygons. We attach servo motors at a scissor link joint, using the servo horn as the offset thickness and connection point between the two layers (Fig. 1D). Specifically, we enclosed each servo in a 3D printed housing (SLS Nylon), which was rigidly attached to the inner shell layer. We 3D print a servo horn (VeroWhite, Objet Connex 260) to couple directly to the outer shell layer. Standoffs between each non-actuated connection point ensure that the servo horn’s offset is held constant throughout the entire system.

This design of the servo drive enables the servos to change the relative angle of the two layers and drive them through their auxetic trajectories. This direct drive of the auxetic trajectory’s angle to control the structure’s expansion is more efficient than needing to drive the motion through a leadscrew or 3D printed mechanism.

Due to the slop in the joints, we needed to use multiple servos to transmit sufficient torque throughout the entire structure. To achieve consistent expansion across the entire shell, we placed two Hitec D89MW servos on opposite poles from one another and programmed them to rotate in sync with one another. Although theoretically, sufficiently small servos could be placed between each bi-layer connection point, we found that our antipodal servos placement offered a good trade-off between assembly complexity, speed, and efficient torque application. This simple actuation design also gives us a significant amount of extra space within the shell, allowing us to potentially place more sensors and power sources within the voxel.

Since the servos provide the bulk of the voxel's internal contents, we used them and their housings as the mechanical foundation to build the rest of the electronics around. One of the servo housings carries the battery (7.4 V 250 mA h) and a switching 6 V regulator (Pololu D36V28F6), while the other carries a wireless microcontroller (Particle Photon). These electronics are mounted on two custom PCBs which simplify wiring and contain protection circuitry for the servos (Fig. 1C). The two boards are then electrically connected together through a 6 wire cable. Controlling the voxel's expansion was relatively straightforward as the auxetic shell only had a single DoF. After connecting to a voxel, the only primitive available is how many degrees the two servos should turn to. The mechanical design of the shell means that servo movement directly translates to the cell's expansion, thus providing a simple command to control volume as an idealized voxel.

III. VOXEL CHARACTERIZATION

To characterize how effectively each robot acted as a voxel, we evaluated expansion ratio, behavior under load, effective stiffness, and blocked force output (Fig. 2).

Diameter measurements were taken by actuating the servos of the voxel in 5 degree increments from its fully closed state, with 45 degrees from closed deemed the fully open state and measuring the outside diameter with a pair of calipers. Reported values are from conducting this test three times for one robot. Our robots achieve an expansion ratio of $1.57 \times$ rather than the theoretical maximum expansion ratio of $1.77 \times$, ranging from a closed diameter of 92 ± 1.2 mm to an open diameter of 144 ± 1.6 mm. This lower measured expansion ratio is expected because of the tab modifications made to the bi-layer design in order to prevent the degenerate case. Having direct servo drive of the scissor joints means that it takes only 0.2 s to move from the fully closed to the fully open state, or 260 mm/s, enabling a wide range of fast dynamic actions. This is significantly faster than other soft robotic modules, such as [5] (260 mm/s) and [10] (1.3 mm/s), increasing the number of applications available to our system.

Load measurements were taken using an Instron 3344 Universal Testing Machine through 3D printed adapters that were bolted directly onto the shell. Blocked force tests were measured by placing the closed voxel within the Instron

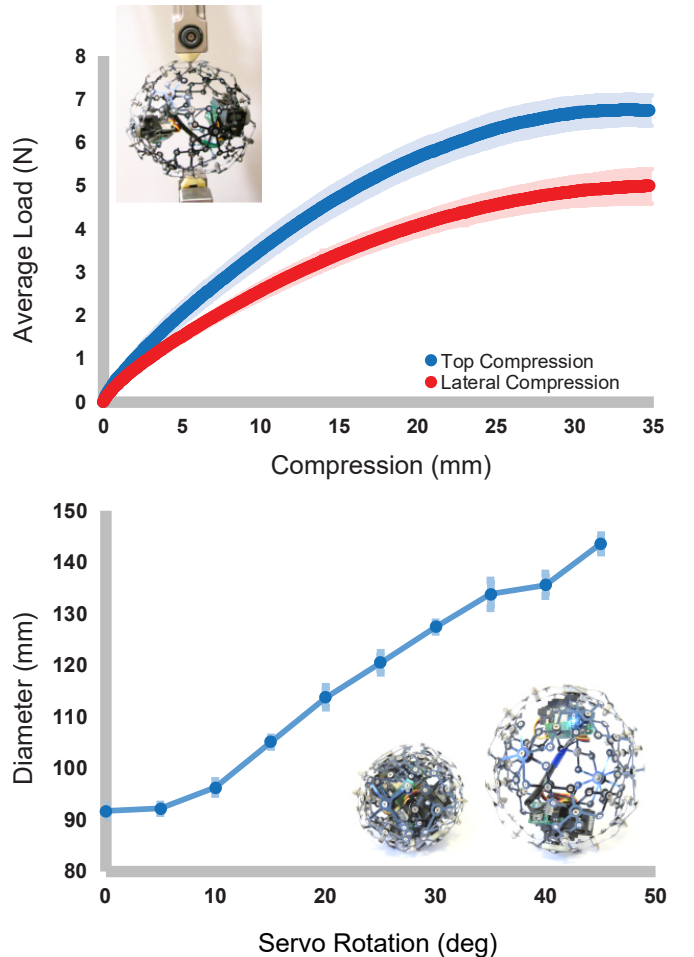


Fig. 2. (Top) Plot demonstrating the average force an individual AuxSwarm voxel can push out under compression when fully open. Top compression is when compression is aligned against the servos' pole while lateral compression is along the equator, as seen in the inset. Error bars reflected standard deviation after 8 tests. (Bottom) Plot presenting how the voxel's diameter changes with servo rotation angle. Error bars reflect standard deviation after 3 tests.

and setting it to actuate to fully open. Reported values are from conducting this test across four different voxels. Compression tests were run at 0.25 mm/s with the voxel powered on at full expansion until 35 mm of compression, about 25% of the overall diameter. Reported values are from conducting this test once across eight different voxels for each orientation. Effective stiffnesses are calculated by measuring the slope of a linear regression from 0 to 20 mm.

Stiffness measurements were taken both along the axis of the servos (top-loading) as well as perpendicular to the servo axis (lateral-loading). We focused load characterizations on the voxel's fully open state as compression tests in the closed states would effectively be the stiffness of the internal servos pressed up against one another due to the compactness of the closed state. This can be seen by the flattening curve in Fig. 2-Top as the compression has finished collapsing the shell and is now working on compressing the servos themselves.

We measured an effective top-loaded stiffness of 388 ± 41 N/m and an effective laterally-loaded stiffness of 280 ± 20 N/m. Despite being made of steel, the voxel's stiffness is

comparable to other soft systems like [20], which reports a stiffness between 108 to 5654 N/m. This is to be expected as the antipodal servos in our design are not connected by any internal structural supports, so there is no extra stiffness to support the structure as a whole beyond the shell. In essence, our structure has about the same stiffness as the flexural modulus of spring steel, which is very low.

The anisotropic difference in stiffness results from the servo layout. The servos' applied torques can help the structure maintain its shape in the axis-aligned direction (at the risk of servo burnout), but not as much when laterally loaded. This analysis is corroborated by the blocked force measurements, which finds that a robot is able to present a blocked force of 8.92 ± 0.17 N along the servo drive axis, but is only able to provide a lateral blocked force of 3.02 ± 0.46 N. Overall, these voxels sacrifice force and load capacity for a larger expansion ratio at a fast speed, making it ideal as the basis for a compliant metamaterial.

IV. AUXSWARM COORDINATION AND MODELING

To compose the voxels into an AuxSwarm, we placed individual robots into a cubic lattice formation (Fig. 3D). To maintain compliance, we chose jointed connections that allowed rotation and limited tilting. We accomplished this by bolting 3D-printed one axis gimbals to the relevant faces of each voxel. The bolt did not restrict rotational motion on the shell, effectively giving us two degrees of freedom for each joint.

Given this joint, we needed to understand what shapes a larger AuxSwarm could achieve. Let r be the radius of a fully contracted voxel. When expanded, the radius increases to kr , with $k > 1$. It is clear that the possible surface profiles we could achieve with a single AuxSwarm layer lie within the plane of $z = r$ and $z = kr$, depending on whether all of the voxels are contracted or expanded, respectively. To understand intermediate curvatures, we develop a model by analyzing the case of a fully contracted voxel connected to a fully expanded voxel (Fig. 3A). This interplay will serve as the fundamental unit of curvature, which can then be repeated for more complex configurations (Fig. 3B).

We start from two contracted voxels on the ground, connected by a gimbal joint. We assume that the size of this joint is negligible to the entire system and instead treat the joint as a point of tangency. We assume the voxel expands through a radial force F outwards, which applies evenly to the entire voxel. This is a valid assumption as we intentionally designed the voxel's auxetic shell to have a trajectory that lies within the 3D point group family. Since the second voxel expands symmetrically outwards, it maintains tangency with the other voxel at all times via the joint connection (although the point of tangency shifts). This is accomplished in real life by the gimbal joint bending and rotating to accommodate the growing size of the second voxel. These joints were designed so that the joint's range of travel is larger than the point where the two voxels touch, making joint limits a non-issue. When the expansion is completed, we achieve

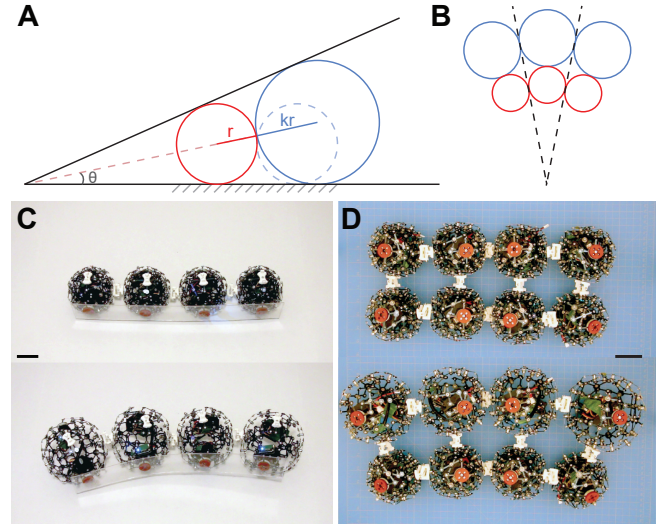


Fig. 3. (A) Schematic of a contracted voxel connected to an expanded voxel, the building block for understanding more complex curvatures that can be created by an AuxSwarm. (B) Demonstration of how (A) can be tiled to model more complex behaviors via symmetry, such as curvature bending. (C) Demonstration of one-dimensional bending under a static constraint layer analogous to pneunet-style soft robotic bending. (D) A version of the same behavior can be seen by using a two-dimensional configuration of voxels, using one layer of auxetic cells to serve as the constraint layer instead of an external boundary. Scale bars are 5 cm.

the final position shown in Fig. 3A. We are interested in the angle formed by the line of tangency between the two voxels and the ground plane as this provides the maximum angle of incline that can be achieved between two voxels (since we can simply decrease the size of the second voxel in order to get a shallower angle).

Let θ be the angle formed by extending the line between the two voxels' centers to where it intersects the ground plane. We know that this center line bisects the overall angle of interest since we can form two congruent triangles above and below the line. We also know that the right triangle formed by the centers of the voxels is similar to the right triangle formed by the extended center line. Thus, by trigonometric relations, we can express θ in terms of r by trigonometric relations as

$$\sin \theta = \frac{kr - r}{kr + r} = \frac{k - 1}{k + 1} \quad (1)$$

Solving for θ , the overall angle of the tangent line is

$$2\theta = 2 \arcsin \frac{k - 1}{k + 1} \quad (2)$$

To answer the original premise, if we want to achieve a surface described by function f within the envelope of $z = r$ and $z = kr$ in a single AuxSwarm layer, we first discretize f into $2r \times 2r$ sections, as this is the minimum size of each voxel. Then, we take ∇f at each point, which will serve as our 2θ for our model. This allows us to solve for an expansion ratio k' , with $1 < k' < k$, which will determine how much we should command the voxel at that point to expand.

From this building block, we can describe many other kinds of AuxSwarm behaviors since all interactions can be

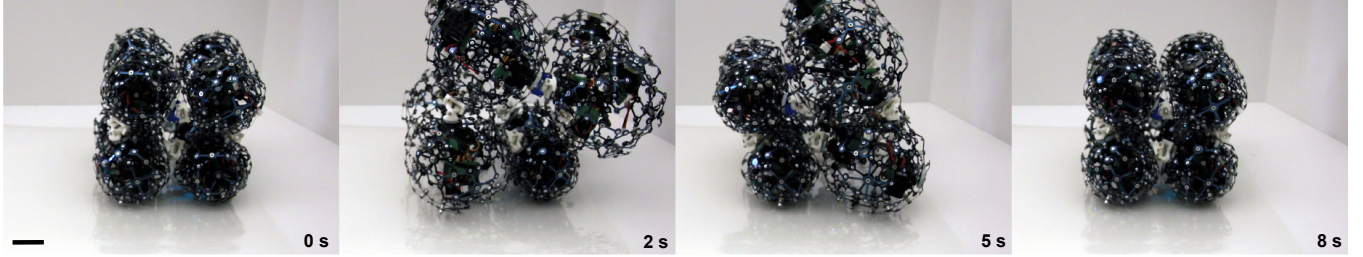


Fig. 4. Demonstration of how a $2 \times 2 \times 2$ AuxSwarm cube can generate a simple rocking locomotion cycle through shifting the overall AuxSwarm's center of mass. Scale bar is 5 cm.

described as being between two voxels. For example, if we were to consider what the overall shape of a bending material would be, the symmetric expansion assumption tells us that lines of symmetry would be preserved for each pair of contracted-expanded voxels (Fig. 3B). We assume that each voxel applies an identical force of F outwards during expansion, meaning the other expanding voxels will match the force of the center voxel. This preserves symmetry and allowing us to just apply our initial model in a tiled manner to understand the overall curvature formed.

We can use Eq. 1 to calculate the overall radius of curvature R of this configuration. From Fig. 3, we derive R trigonometrically as

$$\sin \theta = \frac{kr}{R - kr}$$

Substituting Eq. 1 for $\sin \theta$ and solving for R ,

$$R = \frac{2k^2r}{k - 1} \quad (3)$$

This derivation also highlights how critical the expansion ratio is for any system built off of volumetric actuators. $2 \arcsin \frac{k-1}{k+1}$ has a fairly steep approach to its asymptote of π , meaning that any slight change in the expansion ratio will result in a significant change in what angle can be achieved. Indeed, prior work's expansion ratio of $k = 1.2$ would give a tangent line with angle 10° , while $k = 1.5$ leads to a tangent line with angle 23° . This sharp difference has dramatic implications for what surfaces can be formed through our AuxSwarm.

V. RESULTS

To evaluate AuxSwarms as modular robots, we conduct planar bending and 3D locomotion. For all demonstrations, we pre-configure the voxels into a lattice structure to match the desired AuxSwarm size.

First, we investigate how a $2 \times 4 \times 1$ AuxSwarm curves, both with and without an external constraint layer. This is similar to the soft robotic bending seen in [21], making this a good test to see how AuxSwarm compares to other compliant materials. As a one-dimensional test, we form a $1 \times 4 \times 1$ AuxSwarm, attaching a polycarbonate constraint layer to rubber caps placed at each auxbot's pole. We then form a $2 \times 4 \times 1$ AuxSwarm, using the second layer as a constraint layer (Fig. 3C-D).

These two cases had very similar radii of curvatures. The constrained example had a radius of curvature of 63 cm, while the unconstrained case had a radius of curvature of 55 cm. Normalizing to the unactuated body length of the full AuxSwarm (51 cm), the constrained case curves to a radius of curvature of 1.23 body lengths, while the unconstrained case curves to a radius of curvature of 1.08 body lengths. This is roughly equivalent to a pneu-net style actuator's radius of curvature when actuated at low pressures (0.94–1.5 body lengths), but not at high pressures (0.25 body lengths) [22]. The fact that the AuxSwarm without any constraint layers performed so similarly offers a lot of promise for AuxSwarms acting in complex controllable fashion, no matter the size. This is further corroborated by the fact that we can see the same bending motion even when we disable one of the voxels. As seen in the supplemental video, we are able to see the same overall effect in a repeatable manner, despite a 25% failure in structure with only a minor effect to radius of curvature (53 mm)

However, we note a large discrepancy between what our model predicted and the actual performance. From Sec. III, we have $r = 45.9\text{mm}$ and $k = 1.57$, so by Eq. 3, $R = 39\text{cm}$. However, in actual performance, the voxels in this case only expanded to a diameter of about 115 mm, rather than our measured maximum diameter of 144 mm as in Fig. 2. This makes $k = 1.25$ which would make $R = 57\text{cm}$, a closer fit to our actual measured value. For more accurate model predictions in the future, either encoders should be placed on the servos to measure the actual amount of expansion or more investigation should be taken to fully account for how surface friction and contact affects the overall diameter of the expanded voxels.

Given AuxSwarm's ability to manipulate its global shape, we now leverage that structural control for locomotion. We adopted a rocking strategy to help shift the cube's center of mass in different directions, as seen in Fig. 4. Expansion of the top layer changed the center of mass in different directions, allowing for momentum and movement to build up. For simplicity, we used a pre-programmed quasi-static motion pattern, sending a command once every 3 seconds, and only varied which auxbots carried out this motion plan.

Even with the synchronization constraints of issuing a command every three seconds, we achieved linear motion of 1.13 mm/s , a similar result to the two-dimensional case. We also performed a 90 degree rotation after 150 seconds with

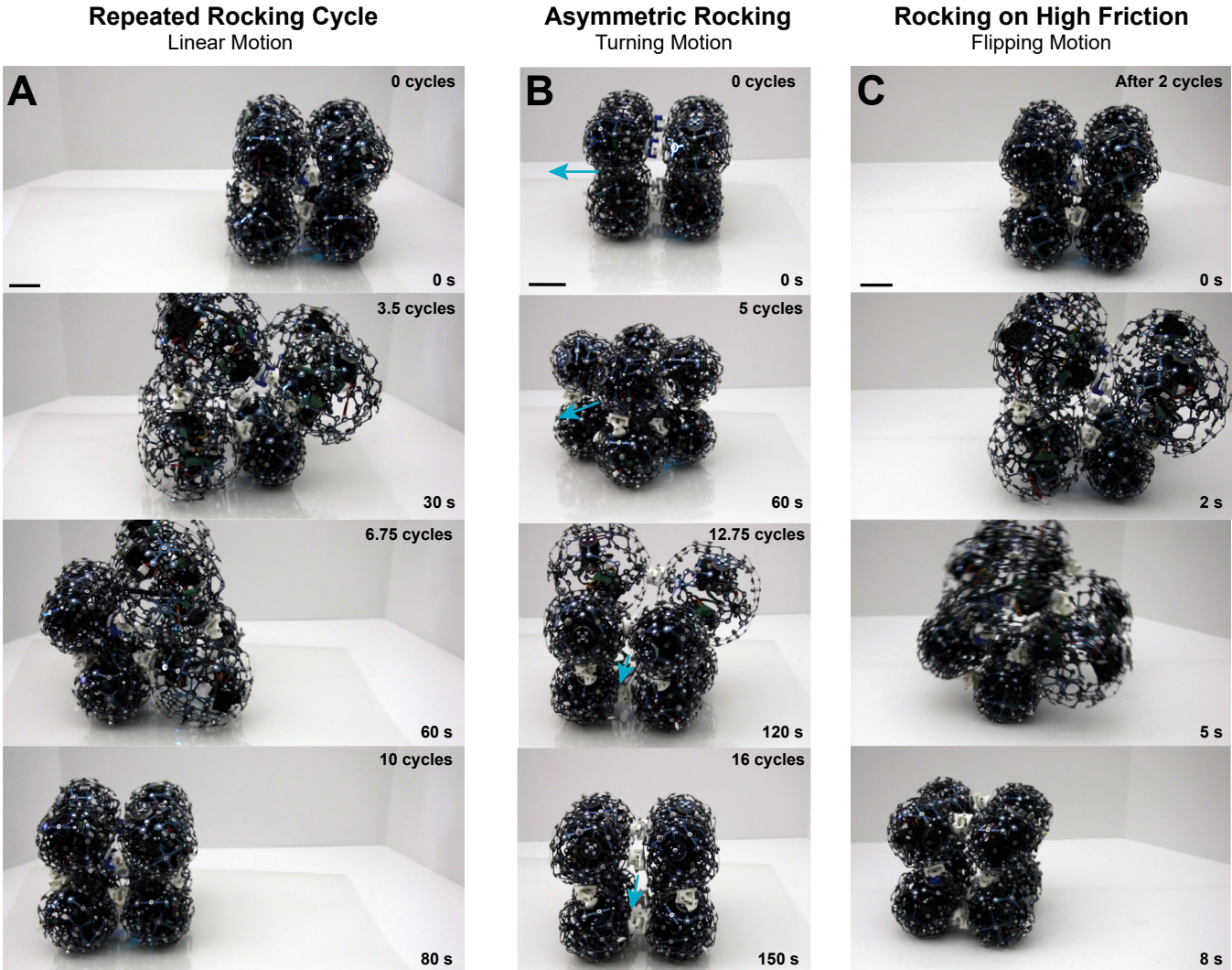


Fig. 5. Through a repeated center-of-mass shifting rocking cycle, a variety of gaits can be achieved for a 3D AuxSwarm configuration. Rocking over a low friction surface results in a (A) linear or (B) a tight turning motion, depending on whether the rocking is symmetric or not. (C) When over a high friction surface, the same rocking motion translates into a flipping motion after sufficient build up. Scale bars are 5 cm.

a turning radius of 60 mm (Fig. 5). We return to the larger radius of curvature as measured in the bending experiments, since the 3D AuxSwarm must serve as its own constraint layer again. Of particular note is the ability to achieve a flipping motion on higher friction surfaces after building up momentum through repeated rocking. This led to much quicker motion as the same 90 mm distance was covered in 24 s, nearly 4 \times faster than by linear shuffling alone. This suggests that our system is versatile enough to adapt for new locomotion patterns across different terrains.

VI. DISCUSSION

In this work, we present AuxSwarm, a modular robotic system that uses volume-changing voxels. AuxSwarm compares favorably against other volume-changing robotic modules. Using our previous literature review (Tab. 4 of [15]), AuxSwarm's voxels are as fast as [5] (0.2 seconds) while expanding more than all systems except [23]. AuxSwarm also moves faster than all previous surveyed work except our own prior results [15]. AuxSwarm was able to achieve these feats

by making intentional decisions to pursue a fast expansion rate and compliance over force capabilities. We demonstrate that modular motorized auxetic units can be used to produce soft cellular materials that are electrically driven, individually addressable, and robust to failure – serving as a unique bridge between modular robotics and soft robotics. We are excited to continue pursuing the possibilities of auxetic geometric design to create more capable versions of programmable matter. Leveraging scalable manufacturing techniques, such as injection molding [24] could lead AuxSwarms to become an ideal platform for programmable matter.

ACKNOWLEDGMENTS

The authors would like to thank James Rowan for help with mathematical modeling. This work was funded through the National Science Foundation EFRI (Grant #1830901) and Amazon. L.C. was supported by the National Science Foundation Graduate Research Fellowship (Grant #1122374) and the Fannie and John Hertz Foundation.

REFERENCES

- [1] M. A. McEvoy and N. Correll, "Materials that couple sensing, actuation, computation, and communication," *Science*, vol. 347, no. 6228, Mar. 2015.
- [2] D. Rus and M. T. Tolley, "Design, fabrication and control of soft robots," *Nature*, vol. 521, no. 7553, pp. 467–475, May 2015.
- [3] J. Seo, J. Paik, and M. Yim, "Modular Reconfigurable Robotics," *Annual Review of Control, Robotics, and Autonomous Systems*, vol. 2, no. 1, pp. 63–88, 2019.
- [4] C. Kopic and K. Gohlke, "Inflatibits: A modular soft robotic construction kit for children," in *Proceedings of the TEI'16: Tenth International Conference on Tangible, Embedded, and Embodied Interaction*, 2016, pp. 723–728.
- [5] A. Vergara, Y.-s. Lau, R.-F. Mendoza-Garcia, and J. C. Zagal, "Soft modular robotic cubes: toward replicating morphogenetic movements of the embryo," *PloS one*, vol. 12, no. 1, 2017.
- [6] C. D. Onal and D. Rus, "A modular approach to soft robots," in *2012 4th IEEE RAS & EMBS International Conference on Biomedical Robotics and Biomechatronics (BioRob)*. IEEE, 2012, pp. 1038–1045.
- [7] M. A. Robertson and J. Paik, "New soft robots really suck: Vacuum-powered systems empower diverse capabilities," *Science Robotics*, vol. 2, no. 9, p. eaan6357, 2017.
- [8] R. M. McKenzie, M. E. Sayed, M. P. Nemitz, B. W. Flynn, and A. A. Stokes, "Linbots: Soft modular robots utilizing voice coils," *Soft robotics*, vol. 6, no. 2, pp. 195–205, 2019.
- [9] C. Zhang, P. Zhu, Y. Lin, Z. Jiao, and J. Zou, "Modular Soft Robotics: Modular Units, Connection Mechanisms, and Applications," *Advanced Intelligent Systems*, vol. 2, no. 6, p. 1900166, 2020.
- [10] M. Devlin, Y. Brad, N. Naclerio, D. A. Haggerty, and E. W. Hawkes, "An Untethered Soft Cellular Robot with Variable Volume, Friction, and Unit-To-Unit Cohesion," in *2020 IEEE/RSJ International Conference on Intelligent Robots and Systems (IROS)*, Oct. 2020, pp. 3333–3339.
- [11] S. Ceron, M. A. Kimmel, A. Nilles, and K. Petersen, "Soft robotic oscillators with strain-based coordination," *IEEE Robotics and Automation Letters*, vol. 6, no. 4, pp. 7557–7563, 2021.
- [12] C. Liu, Q. Lin, H. Kim, and M. Yim, "Smores-ep, a modular robot with parallel self-assembly," *Autonomous Robots*, vol. 47, no. 2, pp. 211–228, 2023.
- [13] A. Abdel-Rahman, C. Cameron, B. Jenett, M. Smith, and N. Gershenfeld, "Self-replicating hierarchical modular robotic swarms," *Communications Engineering*, vol. 1, no. 1, p. 35, 2022.
- [14] J. Lipton, L. Chin, J. Miske, and D. Rus, "Modular volumetric actuators using motorized auxetics," in *2019 IEEE/RSJ International Conference on Intelligent Robots and Systems (IROS)*. IEEE, 2019, pp. 7460–7466.
- [15] L. Chin, M. Burns, G. Xie, and D. Rus, "Flipper-style locomotion through strong expanding modular robots," *IEEE Robotics and Automation Letters*, vol. 8, no. 2, pp. 528–535, 2022.
- [16] L. Zhao, Y. Wu, W. Yan, W. Zhan, X. Huang, J. Booth, A. Mehta, K. Bekris, R. Kramer-Bottiglio, and D. Balkcom, "Starblocks: Soft actuated self-connecting blocks for building deformable lattice structures," *IEEE Robotics and Automation Letters*, vol. 8, no. 8, pp. 4521–4528, 2023.
- [17] H. F. Verheyen, "The complete set of jitterbug transformers and the analysis of their motion," in *Symmetry 2*. Elsevier, 1989, pp. 203–250.
- [18] F. Kovács, T. Tarnai, P. Fowler, and S. Guest, "A class of expandable polyhedral structures," *International journal of solids and structures*, vol. 41, no. 3-4, pp. 1119–1137, 2004.
- [19] F. Kovács, T. Tarnai, S. Guest, and P. Fowler, "Double-link expandohedra: a mechanical model for expansion of a virus," *Proceedings of the Royal Society of London. Series A: Mathematical, Physical and Engineering Sciences*, vol. 460, no. 2051, pp. 3191–3202, 2004.
- [20] W. Gao, J. Kang, G. Wang, H. Ma, X. Chen, M. Kadic, V. Laude, H. Tan, and Y. Wang, "Programmable and variable-stiffness robotic skins for pneumatic actuation," *Advanced Intelligent Systems*, vol. 5, no. 12, p. 2300285, 2023.
- [21] F. Ilievski, A. D. Mazzeo, R. F. Shepherd, X. Chen, and G. M. Whitesides, "Soft Robotics for Chemists," *Angewandte Chemie*, vol. 123, no. 8, pp. 1930–1935, Feb. 2011.
- [22] Y. Sun, Q. Zhang, X. Chen, and H. Chen, "An Optimum Design Method of Pneu-Net Actuators for Trajectory Matching Utilizing a Bending Model and GA," *Mathematical Problems in Engineering*, vol. 2019, p. e6721897, Oct. 2019.
- [23] A. F. Minori, Q. He, P. E. Glick, I. Adibnazari, A. Stopol, S. Cai, and M. T. Tolley, "Reversible actuation for self-folding modular machines using liquid crystal elastomer," *Smart Materials and Structures*, vol. 29, no. 10, p. 105003, 2020.
- [24] B. Jenett, C. Cameron, F. Tourlomousis, A. P. Rubio, M. Ochalek, and N. Gershenfeld, "Discretely assembled mechanical metamaterials," *Science Advances*, vol. 6, no. 47, 2020. [Online]. Available: <https://advances.sciencemag.org/content/6/47/eabc9943>